Numerical Simulations of an Al_2O_3-Water Nanofluid-Based Linear Fresnel Solar Collector

Akpaduado John*, Joseph Oyekale**

* Department of Mechanical Engineering and Mechanics, P.C. Rossin College of Engineering and Applied Sciences, Lehigh University, 27, Memorial Drive West, Bethlehem, PA 18015, USA

* Department of Mechanical Engineering, School of Engineering and Applied Sciences, Federal University of Petroleum Resources Effurun, PMB 1221 Effurun, Nigeria.

Corresponding Author; John Akpaduado; ORCID: 0000-0002-8220-7093, Tel: +1 (835) 240-1884, afj223@lehigh.edu

Second Author: Joseph Oyekale, ORCID: 0000-0003-4018-4660, Tel: +2347033670460, oyekale.oyetola@fupre.edu.ng

Received: 02.08.2022 Accepted: 04.10.2024

Abstract- This study aims to numerically investigate the performance of Al_2O_3-water nanofluid as a heat transfer fluid (HTF) in a linear Fresnel solar receiver. Although a reasonable number of studies have investigated the thermal behaviors of different nanofluids as HTF in solar collectors, the focus has so far been on the parabolic trough collectors, with little or no research efforts available for the linear Fresnel collectors. ANSYS-fluent software was utilized for the simulation in this study, which converted the governing equations to algebraic forms based on the control-volume approach. The Nusselt number and wall temperature were used to characterize the thermal performance of the nanofluid, while the friction factor and eddy viscosity were considered to determine the flow features. The correlation equation proposed by Gnielinski was used to determine the Nusselt number, while the flow features were computed using the Darcy-Weisbach equation. Additionally, the thermal performance of the nanofluid was compared directly with that of pure water. Results showed that the nanofluid improved the thermal performance by about 6-19 % across the solar receiver length. Also, the Nusselt number increases non-uniformly across the length, with a significant rise towards the trailing edge of the nanofluid flow. Conversely, the pressure drop also increases with an increase in the solar receiver length, albeit uniformly. Designers should always factor into the design process to determine the optimum solar collector length when a nanofluid is considered as the HTF; to maximize heat transfer and minimize pressure drop and its attendant economic consequences.

Keywords: Numerical simulation, Nanofluid, Al_2O_3 nanoparticles, Heat transfer analysis, Linear Fresnel collectors, Solar receivers

Nomenclature

Cp	Specific heat, J/kg K
di	Internal diameter of the internal tube, m
do	External diameter of the internal tube, m
f_P	Fiction factor
h	Heat transfer coefficient, W/m2K
k	Thermal conductivity, W/m K
L	Length of tube, m
Nu	Nusselt number
Δp	Pressure drop, Pa
Pr	Prandtl number
v	Fluid velocity, m/s
Al_2O_3	Alumina (aluminum oxide)

Greek letters

ρ	density, kg/m3
μ	dynamic viscosity, kg/ms

1. Introduction

The negative impacts of fossil-fueled energy systems on the environment have necessitated the aggressive focus on clean and renewable energy systems witnessed globally today. Although energy sources such as solar, wind, biomass, hydropower, geothermal, and tidal are mainly on the front burner, other carriers such as hydrogen are also being vigorously explored. In solar energy specifically, several established pathways are available for the exploitation of the thermal energy of the sun, one of which is the Concentrated Solar Power (CSP) route [10]. In CSP systems, collectors are focused on the solar irradiation position by trackers, so that the sun's thermal energy can be accumulated by the heat transfer fluid that flows in the receiver, which is an integral part of the solar collectors. Several practical CSP plants have been built around the world, based on the Parabolic Trough (PT), Linear Fresnel (LF), Solar Tower (Heliostat), and Parabolic Dish technologies [1]. However, solar exploitation is yet to reach a full commercialization stage of development, due to factors such as the transient nature of solar availability, and limitations of heat transfer processes in the solar collectors. Thus, many improvement strategies have been proposed in the literature for decades, and several others are still being proposed to date for the performance enhancement of CSP systems [2–5].

One main strategy for improving the performance of CSP systems that has attracted the attention of energy researchers in recent times is the application of nanofluids for heat transfer enhancement in the collectors [6]. Nanofluids are suspensions of metallic or nonmetallic nanoparticles in a base fluid. They have been explored over the years for use in different sectors of the global economy, but their applications for heat transfer enhancement in renewable energy systems are quite recent [7]. Specifically for the thermal performance improvement of solar collectors which is in focus in this paper, several recent studies are available in the literature, a few of which are critically reviewed in this section. Ashour et al. [4] investigated numerically the thermal performance of ZnO and CuO water nanofluids in a flat-plate solar collector using Egyptian climate conditions. The dedicated 3-D computational fluid dynamics (CFD) model implemented in the study revealed that introducing nanoparticles improved the efficiency of the flat plate solar collector [14-16]. In addition, the study showed that the collector efficiency is influenced by the concentration of the nanoparticles and the heat transfer fluid (HTF) mass flow rate. Similarly, Benabderrahmane et al. [6] analyzed numerically the turbulent forced convection of the dowtherm-A HTF doped with aluminum nanoparticles in a parabolic trough solar receiver. The authors demonstrated that a two-phase model implemented in the study minimizes the need for special correlations to obtain properties of the nanoparticles, relative to a one-phase model. Fahim et al. [8] studied the nanoparticle effects of Cu, Al, and Ti on the thermodynamic performance of thermal oil HTF in parabolic trough solar collectors. They reported that increasing the nanoparticle concentration in thermal oil improved the heat transfer efficiency of the parabolic trough solar collector, with Cu nanoparticles offering the best performance among the three compared. Islam et al. [9] reported similar trends, that a rise in the volumetric concentration of nanoparticles would increase the heat transfer coefficient in parabolic trough solar receivers, based on their joint experimental and numerical study of different nanoparticles. Ying et al.[20] focused on the performance of molten-salt HTF in solar receivers when doped with nanoparticles, and concluded that nanoparticles enhance heat transfer in solar receivers, subject to different concentrations of nanoparticles, inlet velocities of HTF, and heat flux profiles. Abed et al. [1] reported that applications of SiO_2 in Therminol VP-1 as HTF in a parabolic trough solar receiver enhanced performance. However, this enhancement differs in degree for different arrangements of solar inserts into the receiver. Zidan et al. [20] evaluated the performance of 8 different nanoparticles with Therminol VP-1 as HTF in a parabolic trough solar collector hence, reported that TiO_2 yielded the highest enhancement in terms of useful energy, useful exergy, and power block output energy over a year. Additionally, Peng et al. [13] studied the effects of Cu and carbon nanotubes (CNT) on a liquid metal (Gallium) as HTF in a parabolic trough solar receiver. They submitted the addition of nanoparticles enhanced the forced convection heat transfer by about 35-45 %, reduced entropy generation, and increased exergy efficiency; CNT offered a better performance than Cu. However, it was also reported that pressure drop increased in the solar receiver with the introduction of the nanoparticles, relative to what is obtained with pure Gallium. Mahmoudi et al [11] identified CuO-water to offer a better heat transfer enhancement in solar receivers relative to other nanofluids and pure HTF. Mwesigye and Meyer [12] also compared the performance of different nanoparticles in therminol VP-1 as HTF in parabolic trough solar receivers. They highlighted that silver improved the thermal efficiency by about 1.4 percent points over copper, and by about 6.7 percent points over aluminum oxide, with the thermal efficiency increasing with a higher concentration of nanoparticles in therminol VP-1. Babapour et al. [5] experimented with cross-investigating the simultaneous effects of a helically corrugated receiver and nanofluids on the performance of parabolic trough solar collectors. They reported that aluminum nanoparticles increased the Nusselt number by about 220 %, and friction factor by about 146 %, all pointing to the performance enhancement of the parabolic

trough receiver. Subramani et al. [17] reported that a further CNT coating of a copper solar receiver with an Al-based nanofluid would improve heat transfer performance. Vahedi et al. [18] however suggested that the improvement of thermal efficiency of thermal oil-based nanofluids in parabolic trough receivers could be negligibly low with increasing Reynolds number. For some nanoparticles that improved performance, the authors reported that they are barely implementable due to the high cost [19].

In the reviewed literature, applications of nanofluids as heat transfer fluids in solar receivers is a viable performance enhancement strategy. Studies reported in the literature review above were focused on the parabolic trough solar technology. Considering that the performance enhancement of solar receivers is case-specific, as seen from the literature review above, it is necessary to investigate the performance of nanofluids as HTF in other solar technologies. The finding aims to numerically study the performance of a linear Fresnel solar receiver using Al_2O_3-water nanofluid as the heat transfer fluid. To the best of the author's knowledge, the study of Al-based nanofluids as HTF in linear Fresnel collectors remains open in the literature, and this constitutes a valid research gap aimed to be filled in this paper. The specific objectives of the study are:

(i) To quantify the thermal effect of Al_2O_3 in water as heat transfer fluid in a linear Fresnel solar receiver;
(ii) To investigate the behavior of heat transfer parameters such as the surface Nusselt number, thermal conductivity, and wall temperature along the solar receiver length; and
(iii) To analyze the variation of flow features such as friction factor and eddy viscosity along the receiver length.

The methods adopted for numerical analysis in this study are reported in section 2; the main results obtained are discussed in section 3; while the conclusions are summarized in section 4.

2. Methodology

2.1. Simulation Set-up, Assumptions, and Nanofluid Properties

An ANSYS-Fluent model was employed in this study to investigate numerically the thermal performance of Al_2O_3-water nanofluid as HTF in a linear Fresnel solar receiver. The simulation determined the HTF outlet temperature across the length of the receiver tube, at varying volume concentrations of the nanoparticle in the fluid. The control volume-based approach was selected for converting the governing equations to algebraic expressions to be solved numerically. There were 11,634 nodes for the adiabatic wall domain (solid) of the tube; 59,001 nodes for the fluid domain (cell) and 11,634 also for the heater surface domain (solid). The schematic view of linear fresnel solar collector is shown in figure 1.

Standard empirical values of density, specific heat capacity, thermal conductivity, and dynamic viscosity of Al_2O_3 and water were each summed up hence, the average values were employed to determine the Prandtl number (Pr) and the Reynolds number (Re_{Dh}). The steady flow of the nanofluid was assumed a constant speed of 35 m/s. The Reynolds number at the tube entrance is large enough to analyze the flow as turbulent. Hence, the thermophysical properties of the nanofluid are constant. A no-slip heat transfer condition was also assumed (heat flux equals zero). The fluid properties and input parameters for the boundary conditions adopted in this study are highlighted in Tables 1 and 2, respectively. Although to adopt this methodology, the Gnielinski correlation is valid for tubes over a large Reynolds number, Re_{Dh} and Prandtl number, Pr. Such that, $3000 \leq Re_{Dh} \leq 5 * 10^6$ and $0.5 \leq Pr \leq 2000$. Hence, the velocity of the fluid must be 35 m/s and above. The ratio of Al_2O_3 to H_2O is 1:1. The mean of the specific heat capacity C_P in J/kgm^3, density ϱ in kg/m^3, thermal conductivity K in W/m^{2}K, and the dynamic viscosity μ in kg/m.s are considered for the modeling. This is done by adding the value of each thermodynamic property such as specific heat capacity, density, thermal conductivity, and dynamic viscosity of Al_2O_3 and the corresponding values of H_2O; then dividing by two.

Table 1. Fluid Properties

Properties at 30 ^{0}C.	H_2O	Al_2O_3	Nanofluid
S. heat, C_P (J/kgm^3)	4184	451	237.5
Density, ϱ (kg/m^3)	997.1	3970	2486.99
Thermal Cond. (W/m^{2}K)	0.6145	12.12	6.3672
Dynamic μ. (kg/m.s)	0.7972	0.8892	0.8432

Density: the mass fraction of nanofluids in water returns to be x_2 = 0.8 or 80 %, $x_1 = 1 - x_2$, ρ_1 = 997.1 kg/m^3, ρ_2 = 3970 kg/m^3. Where ρ_1 and ρ_2 are the density of H_2O and Al_2O_3.

$$\rho = \frac{1}{\frac{x_1}{\rho_1} + \frac{x_2}{\rho_2}} \quad (1)$$

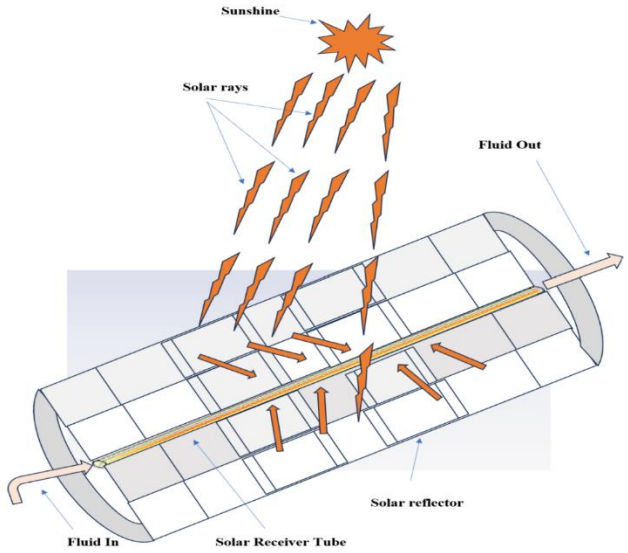

Fig 1. Linear Fresnel solar collector schematic view

Table 2. Input Parameter for Boundary Conditions

Parameter	Value
Pipe outer diameter (m)	0.02
Pipe inner diameter (m)	0.016
Pipe length (m)	1.00
Inlet temperature (^{0}C)	30
Outlet temperature (^{0}C)	30
Inlet velocity (m/s)	63.6
Heat flux (W/m^2)	0 (No-slip condition)
Turbulent intensity	5.063
Pipe material Relative roughness	Steel Commercial Pipe 0.045

Table 3. Steel and Air Properties

Properties at 30 ^{0}C.	Steel	Air
S. heat, C_P (J/kgm^3)	502.416	1.00
Density, 9 (kg/m^3)	8000	1.225
Thermal cond. (W/m^{2}K)	15	0.02225
Dynamic µ. (kg/m.s)	1.793*10^{-3}	1.9*10^{-5}

2.2. Mathematical Correlations

To investigate numerically, the heat transfer performance of Al_2O_3-water nanofluid as HTF in a linear Fresnel solar receiver in this study, the Gnielinski Nusselt number correlation was adopted to predict the thermal profile of the solar receiver. The Gnielinski correlation is valid for tubes over a large Reynolds number range, given by:

$$Nu_{dh} = \frac{(f/8)(Re_{Dh} - 1000)Pr}{1+12.7(f/8)^{1/2}(Pr^{2/3}-1} \quad (2)$$

f is the Darcy friction factor,

$$(0.790 \ln Re - 1.64)^{-2} \quad (3)$$

Validity of Gnielinski correlation;

$$0.5 \leq Pr \leq 2000$$

$$3000 \leq Re_{Dh} \leq 5 * 10^6$$

Dh is the hydraulic diameter in meters, *Re* is the Reynolds number, *Pr* is the Prandtl number, *Nu* is the Nusselt number, and *f* is the Darcy friction factor. The Darcy–Weisbach model was employed to address the friction factors in the analysis. It is expressed in the head loss form as:

$$\Delta H = (f L v^2 \rho)/2D \quad (4)$$

In pressure loss form:

$$\Delta P = (f L v^2 \rho)/2D \quad (5)$$

where Δh is the head loss due to friction (m), Δp is the pressure loss due to friction (Pa), f_D is the Darcy friction factor, L is the pipe length (m), D is the hydraulic diameter of the pipe (m), ρ is the density (kg/m^2), and v is the mean flow velocity.

Osborne Reynolds proposed; Re, = (density * velocity* diameter) /dynamic viscosity

$$Re = (\rho * v * D) / \mu \quad (6)$$

The velocity of flow was chosen to be 63.6m/s. This assertion was discovered theoretically such that with velocity below this value, the flow will not obey turbulent flow, hence Gnielinski correlation validity.

Re = 3001.1.38

The corresponding Prandtl number Pr = (momentum diffusivity/ thermal diffusivity),

$$Pr = (\mu C_P) / K \quad (7)$$

Pr = 306.90

The Darcy friction factor,

$$f = (0.790 \ln Re - 1.64)^{-2} = 0.0455$$

The Moody diagram called the Stanton diagram (known as the Moody chart) validated the friction factor. This is a graph in a non-dimensional form that relates the Darcy–Weisbach friction factor f_D, Reynolds number Re, and surface roughness for fully developed flow in a circular pipe. It was used to predict pressure drop or flow rate down such a pipe.

Relative toughness = (surface roughness/pipe diameter) = ε /D (8)

Where ε is the relative roughness of the pipe and D is the diameter of the pipe. Blasius (1913) proposed that the friction factor can deduced from the equation,

$f = 0.3164\ Re^{-0.25}$ (9)

Blasius also proposed that the friction factor depends on Re, for hydraulically smooth pipe and the turbulent flow, the friction factor formula,

$f = (100.\ Re)^{-0.2}$ (10)

Petuhov concluded in 1970, the friction factor can be achieved from the equation,

$f = (1.82 \log Re - 1.64)^{-2}$ (11)

where the friction factor is obtained to be 0.0455. Also, according to the Sieder-Tate equation for turbulent flow, although this correlation is largely dependent on Re and Pr,

$Nu = 0.023\ R_e^{0.8}\ Pr^{1/3}\ [\mu_{Al2O3} / \mu_{H2O}]^{0.14}$ (12)

Table 3 depicts specific heat capacity values in J/kgm^3, density in kg/m^3, thermal conductivity in W/m^{2}K, and dynamic viscosity in kg/m.s of steel and air at 30 ^{0}C inlet and outlet temperature of $Al2O_3$-water nanofluid in the receiver pipe. Implementing the above equation in ANSYS software made it possible to numerically investigate the thermal energy profile across the length of a linear Fresnel solar receiver when the solar irradiation is focused on it. The Nusselt number and temperatures were used principally to assess the thermal profiles. Also, the flow features were examined across the length of the solar receiver, using the friction factor (pressure loss) and flow viscosity.

3. Results and Discussions

3.1. Mathematical Modeling

The Gnielinski correlation (eqn.1) calculation with a friction factor of 0.0455 depicts that the Nusselt number equals 74.97 and reveals that the Nusselt number increases with an increase in friction factor.

Petukho Nusselt correlation,

$$Nu_{dh} = \frac{(f/8)(Re_{Dh} - 1000)Pr}{1+12.7(f/8)^{1/2}(Pr^{2/3} - 1}$$

Pr > 0.7, $R_e \leq 2300$

Where: $f = (0.790 \ln R_e - 1.64)^{-2}$ with $R_e = 3001.40$ and f = 0.0455, the correlation justifies that the Nusselt number gives the same value as the corresponding Gnielinski correlation (Nu_{dh}= 75.90). Sieder-Tate equation for turbulent flow, although this correlation is highly dependent on Re and Pr,

$Nu = 0.023\ R_e^{0.8}\ Pr^{1/3}\ [\mu_{Al2O3} / \mu_{H2O}]^{0.14}$ where μ is the dynamic viscosity for Al_2O_3 and H_2O

The corresponding Nu = 92.45

Table 4 Pipe Variation Concerning Pressure Head

Length (cm)	Pressure loss	Bar
0.2	25.15 * 10^5	25
0.4	50.30 * 10^5	50
0.6	75.50 * 10^5	75
0.8	100.60 *10^5	100
1.0	12.57 * 10^5	125

Table 4 shows the pressure loss across the length of the solar receiver pipe. The nanofluid obeys the Gnielinski correlation, Pr and corresponding Re_{Dh} of the fluid property are 0.5 ≤ Pr ≤ 2000 and 3000 ≤ Re_{Dh} ≤ 5 * 10^6. Substituting the fluid thermodynamics properties into the pressure head equation, it is observed that the pressure loss increases across as the pipe increases. Hence, the simulation results from the ANSYS fluent also affirmed this as shown in the pressure drop variation across the solar receiver length in Figure 4.

3.2. Thermal Profile of Al_2O_3-Water Nanofluid Across the Solar Receiver Length

As mentioned earlier, the Gnielinski correlation applied made it possible to predict numerically the heat transfer performance of the linear Fresnel solar receiver using Al_2O_3-water nanofluid as the HTF. Al_2O_3-water nanofluid at 30 ^{0}C flows in the solar receiver pipe with a specific heat capacity of 237.5 J/kgm^3, a density of 2486.99 kg/m^3, the thermal conductivity, and dynamic viscosity of the nanofluid flowing at the velocity of 63.6 m/s are 6.3672 W/m^{2}K and 0.8432kg/m.s respectively. The thermal profile of the HTF across the solar receiver surface is presented in Fig. 2 based on the Nusselt number. As can be seen, there is a non-uniform increase in the Nusselt number along the solar receiver length. While the Nusselt number growth is only moderate for about 95 % of the receiver length from the leading edge, the growth turns significantly high at the trailing edge, becoming almost vertical at the end of the pipe. The significance of this is that there exists a non-uniform thermal profile of the Al_2O_3-water nanofluid across the surface of a solar receiver and that the convective heat transfer tends to increase drastically at the trailing edge of the receiver. When pure water was used as HTF for the simulation, results showed that the Nusselt number (and heat transfer

performance) was higher with the use of the applied nanofluid across the length of the receiver, with about 6 – 19 % increase. The ANSYS contours of the entire thermal and flow properties investigated in this study are presented in this paper as an appendix.

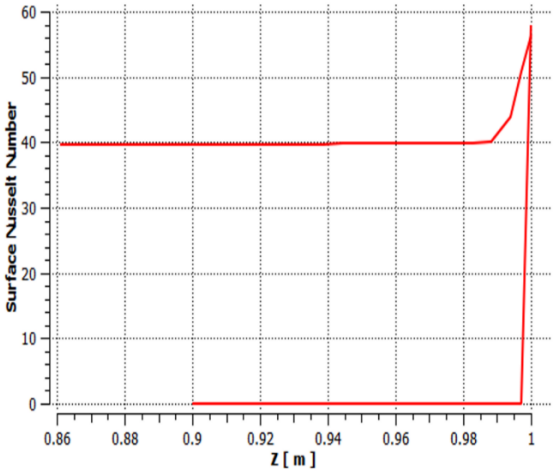

Fig. 2. Surface Nusselt number variation along the solar receiver length

Similarly, the profile of the adjacent wall temperature of the solar receiver is presented in Fig. 3 over the receiver length. As expected, the wall temperature decreases almost linearly from the leading edge to the trailing edge as the nanofluid flows through the solar collector length. This occurs at a constant thermal conductivity of the wall material as shown in Fig. 4. It had been assumed fixed in the simulation set-up.

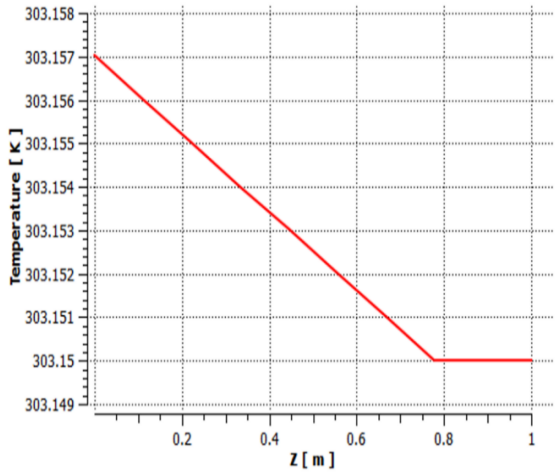

Fig. 3. Wall temperature profile over the length of the solar receiver

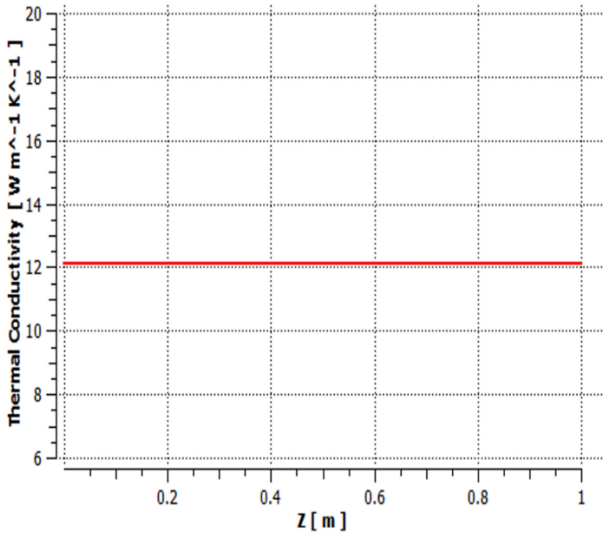

Fig. 4 – Thermal conductivity over the length of the solar receiver

3.3. Flow Features of Al_2O_3-Water Nanofluid Across the Solar Receiver Length

The friction factor measured by pressure drop, and the eddy viscosity, were applied to characterize the flow features of the Al_2O_3-water nanofluid under investigation in this paper for application as HTF in a linear Fresnel solar receiver. Based on the Darcy-Weisbach equation applied in the ANSYS simulation, a trend was obtained for pressure drop variation across the solar receiver length, as shown in Fig. 5. Similarly, the variation of eddy viscosities across the solar receiver length is shown in Fig. 6. As can be seen, increase in solar receiver length also increases the pressure drop, which translates to an increase in friction factor within the flow. This work in contrast relates to the thermal performance illustrated by the Nusselt number in Fig. 2, which increases with an increase in the solar receiver length. These two results imply that due attention must be given to determining the optimum length when applying nanofluid as HTF in a linear Fresnel solar receiver, where the pressure drop would be as low as possible, and the heat transfer coefficient as high as possible. This assertion is corroborated by the result of the eddy viscosity presented in Fig. 6, where the eddy viscosity remains constant over a good distance across the solar receiver, only to ascend drastically towards the trailing edge of the flow. Figure 7 and Figure 8 show the behavior of the Al_2O_3-water nanofluid under the influence of turbulent kinetic energy in square meters per second square ($m^2. s^{-2}$) and the turbulent eddy frequency per second (s^{-1}) across the length of the solar receiver.

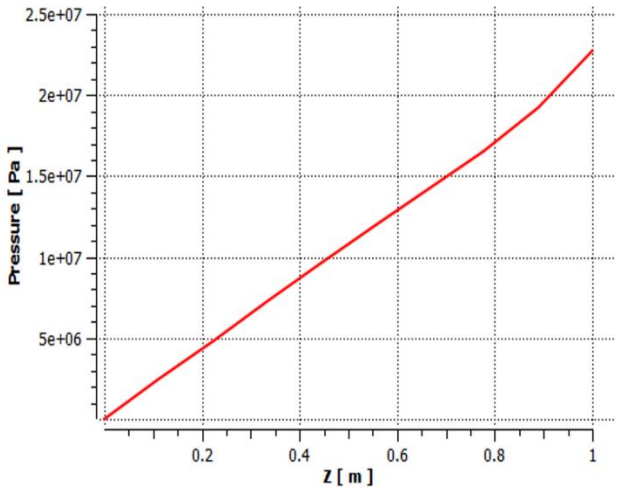

Fig. 5. Pressure drop variation across the solar receiver length

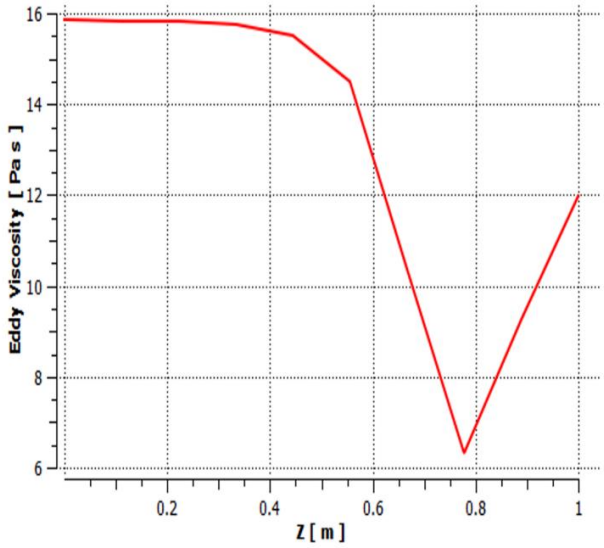

Fig. 6. Effect of receiver length on the eddy viscosity

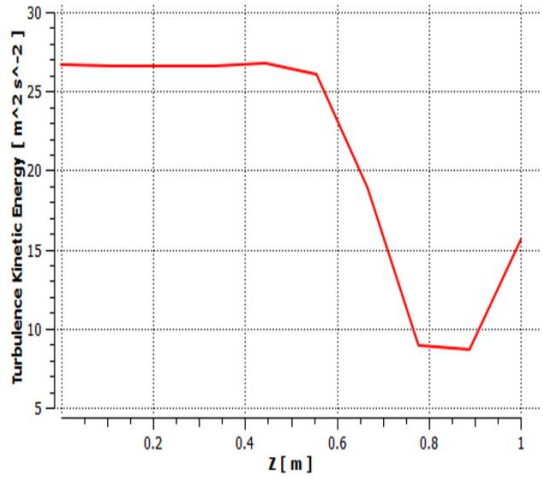

Fig. 7. Turbulent kinetic energy over the length of the solar receiver

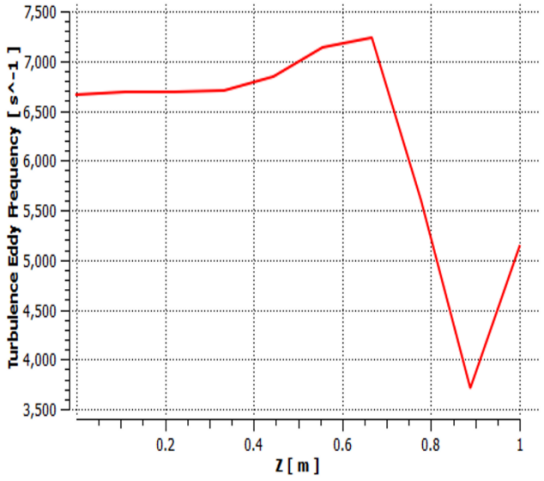

Fig. 8. Turbulent eddy frequency over the length of the solar receiver

Table 5 shows a comparative performance and results of different nanofluids in solar receiver tubes in some reviewed literature. Al_2O_3-water nanofluid as HTF in the solar receiver pipe contours from ANSYS for difference thermal and flow properties which include the pressure, temperature contour, density, velocity, Surface Nusselt Number, surface heat transfer coefficient, skin friction coefficient, thermal conductivity, Al_2O_3-water nanofluid isosurface view, velocity streamline contours, as well as the scale residual of the nanofluid, velocity magnitude against the position in the receiver pipe, and velocity and temperature magnitude contours investigated in the study are shown in Appendix Figure 1 -14 in this paper. Material and absolute roughness property values are also presented in the Appendix Table 1.

Table 5. Comparative nanofluid performance and results with some reviewed works of literature

Reference	Work	Method (s)	Materials	Results
Benabderrahmane et al [6]	Compound heat transfer enhancement numerical analysis using single & two-phase models in PTC receiver	Finite volume method using ANSYS, and K-Ɛ turbulent model.	HTF; nanofluid consisting of Alumina nanoparticles suspended in synthetic oil Dowtherm-A	PTC offers better heat transfer. Darcy friction factor is considerably similar in both single and two-phase modeling
Abed et al [1]	Multiple strips inserts and nanofluids on the thermal-hydraulic performances effect of parabolic trough collectors	Conjugated heat transfers multi-region simple foam (cht Multi Region Simple Foam) engineering tool, Finite-Volume method	Large conical-shaped strips, small conical strips, rectangular-shaped strips, and elliptical-shaped strips. SiO_2 nanoparticles mixed in Therminol® VP-1 (TO)	Nusselt number for large conical strips leads to 57.49 % & 62.53 % for the nanofluid. Thermal conductivity increases to 15.41 %
Carmo Zidan et al [7]	Various nanofluids performance evaluation for parabolic trough collectors	PTC; Parametric Technology Corporation software	Parabolic trough collector, Therminol VP-1, TiO_2	TiO_2 most suitable nanoparticle material to be dispersed in therminol VP-1 for the PTC system.
Ashour et al [4]	Numerical investigation on the thermal performance of a flat plate solar collector	A 3D computational fluid dynamics (CFD) model	water (H_2O), zinc oxide (ZnO) nanofluid, and copper oxide (CuO) nanofluid water-based	H_2O–CuO nanofluid with an average efficiency of about 81.64% at a mass flow rate of 0.0125 kg s^{-1} and VF of 0.15%.
Babapour et al [5]	Helically corrugated receiver and nanofluids PTC; simultaneous effects	ASHRAE standard software (93:2010)	Al_2O_3/water nanofluid at volume fractions of 0.25-1%	An increase of about 219.56% in Nusselt number
This study	Numerical simulations of an Al_2O_3-water nanofluid-based linear Fresnel solar collector	ANSYS Fluent software	Al_2O_3-water nanofluid (Al_2O_3 1:1), linear Fresnel solar collector	Thermal performance increases and the Nusselt number increases by 6-19 % across the pipe length relative to pure water. Friction factors also increase

4. Conclusions

The thermal performance of Al_2O_3-water nanofluid as heat transfer fluid (HTF) in a linear Fresnel solar receiver has been investigated numerically. An ANSYS-Fluent model was adopted to examine the thermal behavior of the nanofluid HTF across the length of the horizontal stainless-steel solar receiver tube. The flow was assumed to be the turbulent flow in the tube with constant properties. The Nusselt number and wall temperature were used principally to investigate the thermal profile of the nanofluid in the solar receiver. Hence the pressure drops and eddy viscosity characterized the flow in the tube. The correlation equation proposed by Gnielinski was used to determine the Nusselt number, while the friction factor was computed using the Darcy-Weisbach equation. The mean of the specific heat capacity C_P in J/kgm^3, density ϱ in kg/m^3, thermal conductivity K in W/m^{2}K, and the dynamic viscosity μ in kg/m.s were considered in the modeling. This is done by adding the value of each thermodynamic property, i.e., specific heat capacity, density, thermal conductivity, and dynamic viscosity of Al_2O_3 and the corresponding values of H_2O; then dividing by two. A direct comparison between the thermal behavior of pure water and the Al_2O_3-water nanofluid showed the potential benefits derived using nanofluid in linear Fresnel solar collector type. The main results obtained from the study are:

- The use of the Al_2O_3-water nanofluid as HTF in a linear Fresnel solar receiver would improve thermal performance (measured by Nusselt number) by about 6-19 % across the length of the receiver, relative to pure water;
- Although the wall temperature decreases almost uniformly along the length of the receiver; the effect of a length on thermal performance is non-uniform, with the highest Nusselt number obtained towards the trailing edge;
- Increasing the length of the receiver resulted in a higher friction factor (measured by pressure drop) for nanofluid flow across the receiver tube.

Lastly, Al_2O_3-water nanofluid as HTF in linear Fresnel should be encouraged due to the potential improvement of the heat transfer performance. Hence, with Al_2O_3-water nanofluid as heat transfer fluid, better efficiency is achievable compared to ordinary water as nanofluid in a solar receiver pipe as proposed in literature. However, the optimum length of the solar receiver that would maximize the heat transfer gain should be determined during design without any extreme increase in the pressure drop and its attendant economic burdens. Contours from ANSYS for the different thermal and flow properties investigated in this study were also presented in the Appendix.

References

[1] Abed, N.; Afgan, I.; Cioncolini, A.; Iacovides, H.; Nasser, A. Effect of various multiple strip inserts and nanofluids on the thermal-hydraulic performances of parabolic trough collectors. *Appl. Therm. Eng.* 2022, *201*, 117798, doi:10.1016/j.applthermaleng.2021.117798.

[2] Ajbar, W.; Parrales, A.; Huicochea, A.; Hernández, J.A. Different ways to improve parabolic trough solar collectors' performance over the last four decades and their applications: A comprehensive review. *Renew. Sustain. Energy Rev.*2022, *156*, doi:10.1016/j.rser.2021.111947.

[3] Al-Oran, O.; Lezsovits, F. Recent experimental enhancement techniques applied in the receiver part of a parabolic trough collector – A review. *Int. Rev. Appl. Sci. Eng.* 2020, *11*, 209–219, doi:10.1556/1848.2020.00055.

[4] Ashour, A.F.; El-Awady, A.T.; Tawfik, M.A. Numerical investigation on the thermal performance of a flat plate solar collector using ZnO & CuO water nanofluids under Egyptian weathering conditions. *Energy* 2022, *240*, doi:10.1016/j.energy.2021.122743.

[5] Babapour, M.; Akbarzadeh, S.; Valipour, M.S. An experimental investigation on the simultaneous effects of a helically corrugated receiver and nanofluids in a parabolic trough collector. *J. Taiwan Inst. Chem. Eng.* 2021, *128*, 261–275, doi:10.1016/j.jtice.2021.07.031.

[6] Benabderrahmane, A.; Benazza, A.; Laouedj, S.; Solano, J.P. Numerical analysis of compound heat transfer enhancement by single and two-phase models in parabolic trough solar receiver. *Mechanika* 2017, *23*, 55–61, doi:10.5755/j01.mech.23.1.14053.

[7] do Carmo Zidan, D.; Brasil Maia, C.; Reza Safaei, M. Performance evaluation of various nanofluids for parabolic trough collectors. *Sustain. Energy Technol. Assessments* 2022, *50*, 101865, doi:10.1016/j.seta.2021.101865.

[8] Fahim, T.; Laouedj, S.; Abderrahmane, A.; Alotaibi, S.; Younis, O. Heat Transfer Enhancement in Parabolic through Solar Receiver : A Three-Dimensional Numerical Investigation. 2022, 1–19.

[9] Islam, M.K.; Hasanuzzaman, M.; Rahim, N.A.; Nahar, A. Effect of nanofluid properties and mass a -flow rate on heat transfer of o parabolic -trough concentrating solar system.

J. Nav. Archit. Mar. Eng. 2019, *16*, 33–44, doi:10.3329/jname.v16i1.30548.

[10] Kumaresan, G.; Sudhakar, P.; Santosh, R.; Velraj, R. Experimental and numerical studies of thermal performance enhancement in the receiver part of solar parabolic trough collectors. *Renew. Sustain. an Energy Rev.* 2017, *77*, 1363–1374, doi:10.1016/j.rser.2017.01.171.

[11] Mahmoudi, A.; Fazli, M.; Morad, M.R.; Gholamalizadeh, E. Thermo-hydraulic performance enhancement of nanofluid-based linear solar receiver tubes with forward perforated ring steps and triangular cross-section; a numerical investigation. *Appl. Therm. Eng.* 2020, *169*, 114909, doi: 10.1016/j.applthermaleng.2020.114909.

[12] Mwesigye, A.; Meyer, J.P. Optimal thermal and thermodynamic performance of a solar parabolic trough receiver with different nanofluids and at different concentration ratios. *Appl. Energy* 2017, *193*, 393–413, doi:10.1016/j.apenergy.2017.02.064.

[13] Peng, H.; Guo, W.; Li, M. Thermal-hydraulic and thermodynamic performances of liquid metal based nanofluid in parabolic trough solar receiver tube. *Energy* 2020, *192*, 116564, doi:10.1016/j.energy.2019.116564.

[14] Răboacă, M.S.; Badea, G.; Enache, A.; Filote, C.; Răsoi, G.; Rata, M.; Lavric, A.; Felseghi, R.-A. Concentrating Solar Power Technologies. *Energies* 2019, *12*, 1048, doi:10.3390/en12061048.

[15] Sandeep, H.M.; Arunachala, U.C. Solar parabolic trough collectors: A review on heat transfer augmentation techniques. *Renew. Sustain. Energy Rev.* 2017, *69*, 1218–1231, doi:10.1016/j.rser.2016.11.242.

[16] Souza, R.R.; Gonçalves, M.; Rodrigues, R.O.; Minas, G.; Miranda, J.M. Recent advances on the thermal properties and applications of nanofluids : From nanomedicine to renewable energies. 2022, *201*, doi: 10.1016/j.applthermaleng.2021.117725.

[17] Subramani, J.; Sevvel, P.; Anbuselvam; Srinivasan, S.A. Influence of a CNT coating on the efficiency of a solar parabolic trough collector using AL2O3 nanofluids - A multiple regression approach. *Mater. Today Proc.* 2021, *45*, 1857–1861, doi:10.1016/j.matpr.2020.09.047.

[18] Vahedi, B.; Golab, E.; Nasiri Sadr, A.; Vafai, K. Thermal, thermodynamic and exergoeconomic investigation of a parabolic trough collector utilizing nanofluids. *Appl. Therm. Eng.* 2022, *206*, 118117, doi: 10.1016/j.applthermaleng.2022.118117.

[19] Wole-osho, I.; Okonkwo, E.C.; Abbasoglu, S.; Kavaz, D. *Nanofluids in Solar Thermal Collectors: Review and Limitations*; Springer US, 2020; Vol. 41; ISBN 0123456789.

[20] Ying, Z.; He, B.; Su, L.; Kuang, Y.; He, D.; Lin, C. Convective heat transfer of molten salt-based nanofluid in a receiver tube with non-uniform heat flux. *Appl. Therm. Eng.* 2020, *181*, doi: 10.1016/j.applthermaleng.2020.115922.

APPENDIX: CONTOURS

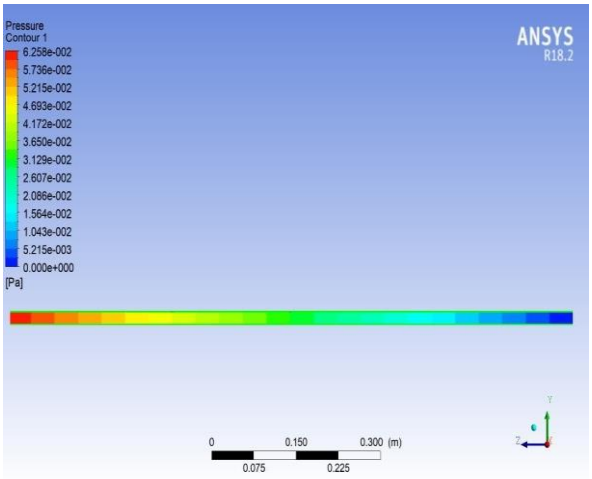

Appendix Fig 1. Pressure contour effect on Al_2O_3-water nanofluid in the Receiver Pipe

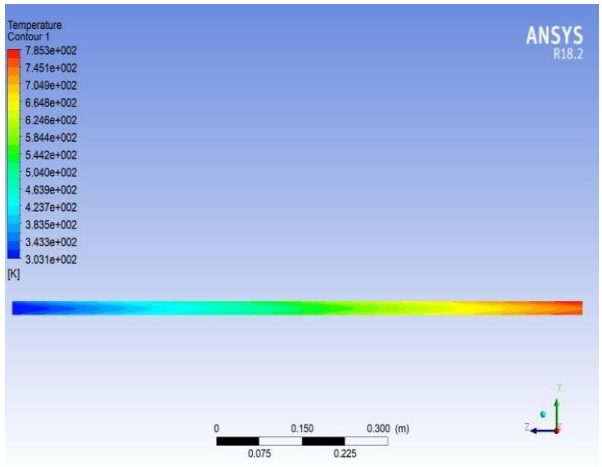

Appendix Fig. 2. Temperature contour on Al_2O_3-water nanofluid in the Receiver Pipe

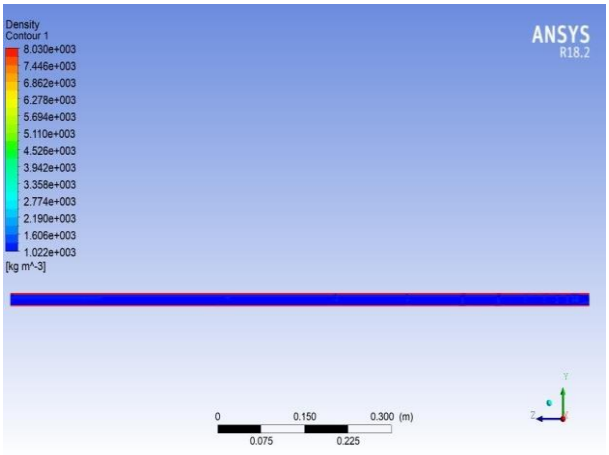

Appendix Fig. 3. Density contour effect on Al_2O_3-water nanofluid in the Receiver Pipe

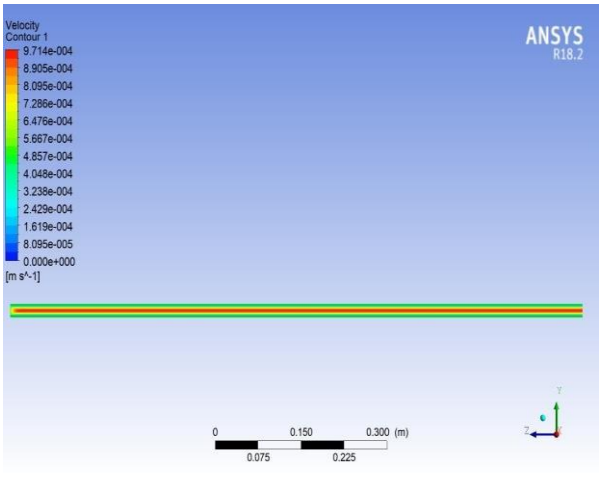

Appendix Fig 4. Velocity contour on Al_2O_3-water nanofluid in the Receiver Pipe

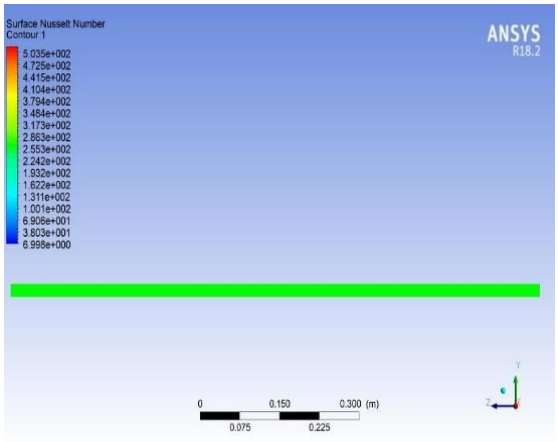

Appendix Fig. 5. Surface Nusselt Number contour on Al_2O_3-water in the Receiver Pipe

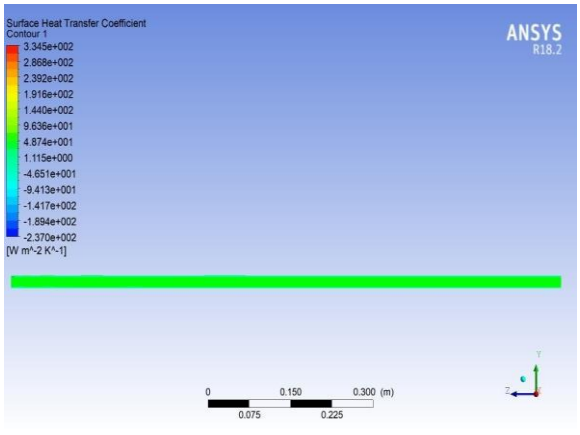

Appendix Fig. 6. Surface Heat transfer coefficient contour on Al_2O_3-water in the Receiver Pipe

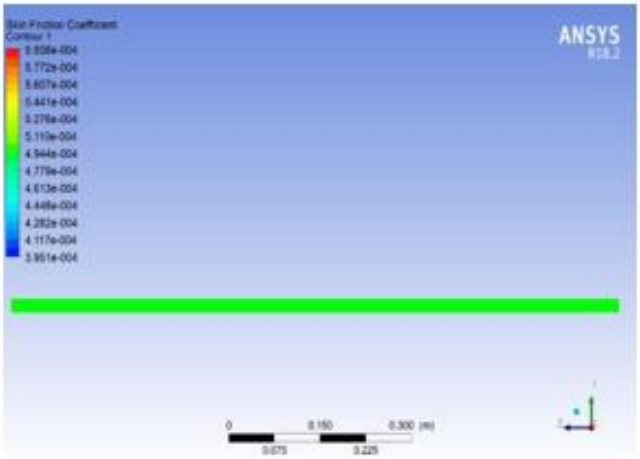

Appendix Fig. 7. Skin Friction Coefficient contour on Al_2O_3-water in the Receiver Pipe

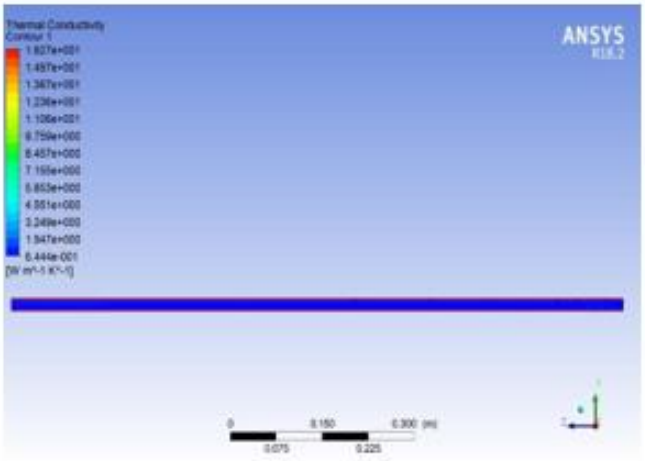

Appendix Fig. 8. Thermal Conductivity Contour on Al_2O_3-water in the Receiver Pipe

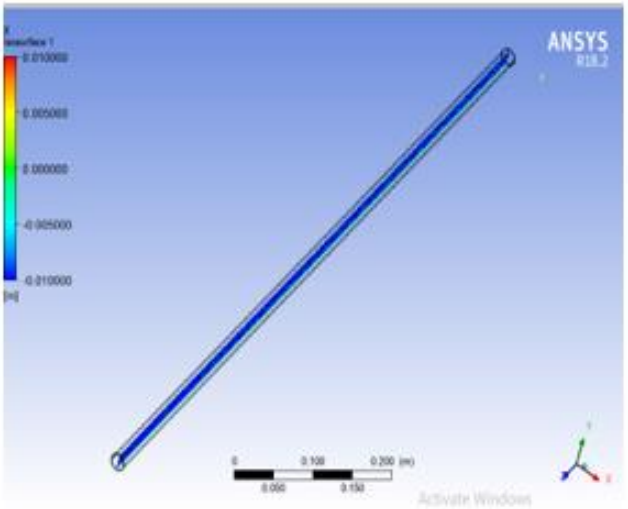

Appendix Fig. 9. Isosurface behavior of Al_2O_3-water in the Receiver Pipe

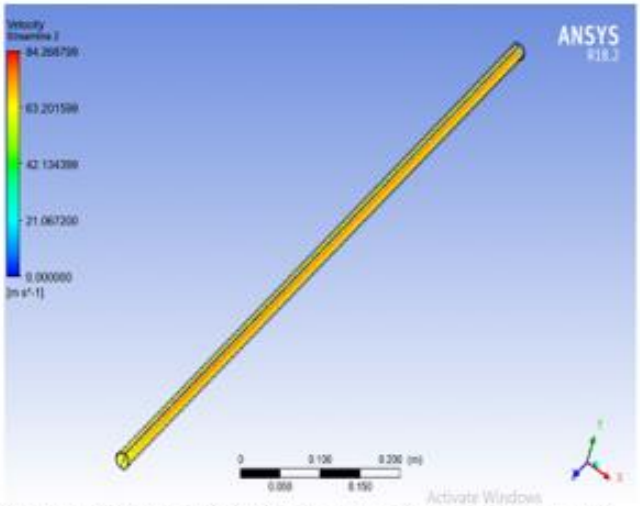

Appendix Fig. 10. Velocity Streamline behavior of Al_2O_3-water in the Receiver Pipe

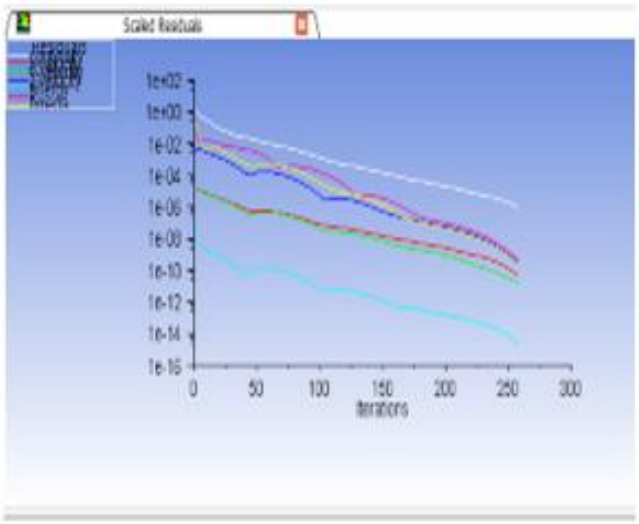

Appendix Fig. 11. Al_2O_3-water nanofluid Scale Residuals in the Receiver Pipe

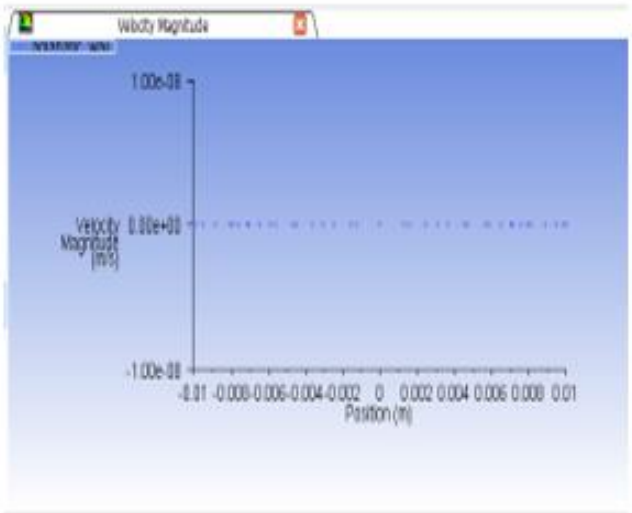

Appendix Fig. 12. Al_2O_3-water nanofluid Velocity Magnitude against Position in the Pipe

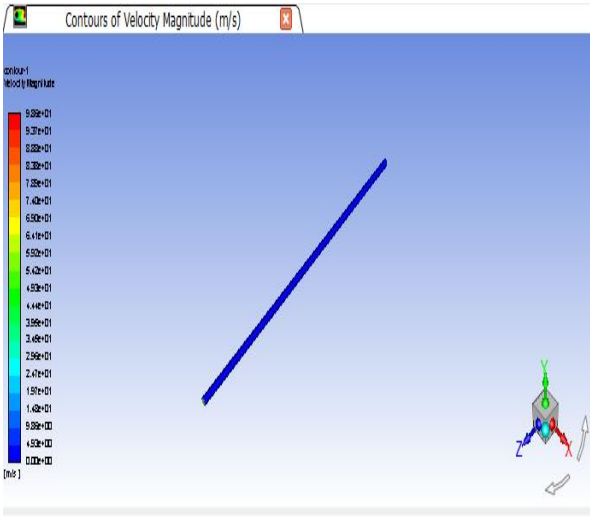

Appendix Fig. 13. Contours of Velocity Magnitude in the Receiver Pipe

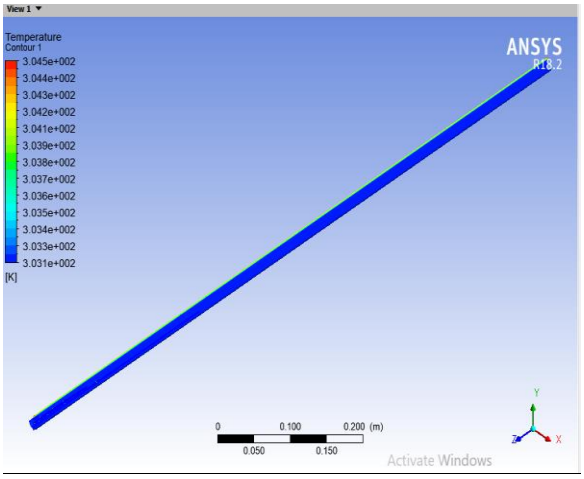

Appendix Fig. 14. Contours of Temperature Magnitude in the Receiver Pipe

Appendix Table 1. Material and Absolute roughness values table

Material	Absolute Roughness (mm)
Copper, Lead, Brass, Aluminum (new)	0.001 - 0.002
PVC and Plastic Pipes	0.0015 - 0.007
Flexible Rubber Tubing - Smooth	0.006-0.07
Stainless Steel	0.0015
Steel Commercial Pipe	0.045 - 0.09
Weld Steel	0.045
Carbon Steel (New)	0.02-0.05
Carbon Steel (Slightly Corroded)	0.05-0.15
Carbon Steel (Moderately Corroded)	0.15-1
Carbon Steel (Badly Corroded)	1-3
Asphalted Cast Iron	0.1-1
New Cast Iron	0.25 - 0.8
Worn Cast Iron	0.8 - 1.5
Rusty Cast Iron	1.5 - 2.5
Galvanized Iron	0.025-0.15
Wood Stave	0.18-0.91
Wood Stave, used	0.25-1
Smoothed Cement	0.3
Ordinary Concrete	0.3 - 1
Concrete – Rough, Form Marks	0.8-3